CFD modelling of sampling locations for early detection of spontaneous combustion in long-wall gob areas

Liming Yuan* and Alex C. Smith

Office of Mine Safety and Health Research,
National Institute for Occupational Safety and Health (NIOSH),
P.O. Box 18070, 626 Cochrans Mill Road,
Pittsburgh, PA 15236, USA
E-mail: Lcy6@cdc.gov
E-mail: Aos6@cdc.gov
*Corresponding author

Abstract: In this study, computational fluid dynamics (CFD) modeling was conducted to optimize gas sampling locations for the early detection of spontaneous heating in longwall gob areas. Initial simulations were carried out to predict carbon monoxide (CO) concentrations at various regulators in the gob using a bleeder ventilation system. Measured CO concentration values at these regulators were then used to calibrate the CFD model. The calibrated CFD model was used to simulate CO concentrations at eight sampling locations in the gob using a bleederless ventilation system to determine the optimal sampling locations for early detection of spontaneous combustion.

1 Introduction

Spontaneous combustion is a serious fire hazard for US underground coal mines, especially for western mines where the coal is generally of lower rank. Although there were no reported fatalities directly attributed to spontaneous combustion in US coal mines in last decade, the potential for a spontaneous combustion event leading to an explosion still exists, especially in mines with substantial amounts of methane. Although the spontaneous combustion tendencies of coals in the western US have been well characterised, spontaneous heatings still occur because of complicated interactions between ventilation airflow, geological conditions and mining practices. In the US, most underground coal mines utilise bleeder ventilation systems to prevent methane buildup in gob areas. For mines with a demonstrated history of spontaneous combustion, bleederless ventilation systems that can serve to control spontaneous combustion are often approved by the US Mine Safety and Health Administration (MSHA). Regardless of the ventilation scheme employed, the early detection of spontaneous heating is critical in the prevention and control of fires caused by spontaneous combustion in underground coal mines.

The primary method used for the detection of spontaneous combustion in underground coal mines is the early detection of low levels of gaseous products of coal oxidation most often through the use of in-mine continuous gas analysers using a tube bundle gas sampling system although gas samples can also be obtained for laboratory analysis by gas chromatography. The gaseous products of low-temperature coal oxidation occurring at the very early stages of a self-heating are carbon monoxide (CO), carbon dioxide (CO_2) and water (H_2O). Methane (CH_4), hydrogen (H_2) and other low–molecular weight hydrocarbons are released as the coal temperature rises. Chamberlain and Hall (1973) found that CO is the most sensitive indicator of the early stages of coal oxidation and the continuous monitoring of this gas provides the earliest detection of self-heating. Other gases have also been investigated, such as CO_2, CH_4, H_2 and higher hydrocarbons. CO_2 production increases with increasing temperature and is useful in determining the state of a fire. However, several sources of CO_2 may be present in mines, making its use unreliable. CH_4 is usually present in large background quantities and, as with H_2 and other hydrocarbons, is not produced until much higher coal temperatures are reached. Cliff et al. (2000) conducted large-scale tests to evaluate detection and monitoring methods of spontaneous combustion of coal. They found that the best indicators of spontaneous combustion are those that are independent of airflow, such as the amount of CO released and Graham's ratio, but that even these indicators have some limitations. Chakravorty and Woolf (1979) found that the absolute level of CO in the mine air, whether high or low (within reasonable bounds), is not of great significance but that an increasing trend is indicative of heating. In the US, monitoring the trend of CO concentration in the mine atmosphere is the most widely used method for detecting the occurrence of spontaneous combustion (Mitchell, 1996).

Long-wall gobs can be of vast extent and the effectiveness of early detection of spontaneous heating in these gob areas can be greatly improved by the careful selection of locations for gas sampling. Selecting optimum gas sampling locations would enable the mine operator to detect heatings early and to determine the most probable location of the heatings. If locations of gob heatings could be pinpointed accurately, more effective prevention and control measures, such as nitrogen injection, could be employed.

In this paper, the gas data collected from a western coal mine long-wall panel with a bleeder ventilation system during a spontaneous heating event were utilised to calibrate and validate the Computational Fluid Dynamics (CFD) model developed for the simulation of spontaneous heating in long-wall gob area (Yuan and Smith, 2007; Smith and Yuan, 2008). The CFD model was then used to investigate optimum location strategies for the early detection of spontaneous heating in long-wall gob areas with a bleederless ventilation system. This paper presents the results of these measurements and subsequent analyses.

2 Long-wall panel layout and ventilation system

Figure 1 shows the layout of the long-wall panel and the bleeder system configuration, including ventilation quantities. The gob area is 300 m (1000 ft) long, 375 m (1250 ft) wide and 10 m (33 ft) high starting from the bottom of the coal seam. The ventilation airways are 3 m (10 ft) high and 6 m (20 ft) wide. There are four regulators, designated as R1, R2, R3 and R4, respectively, on the tailgate side and four regulators, designated as R5, R6, R7 and R8, respectively, on the back end of the panel.

Figure 1 Layout of original long-wall panel with bleeder ventilation system (see online version for colours)
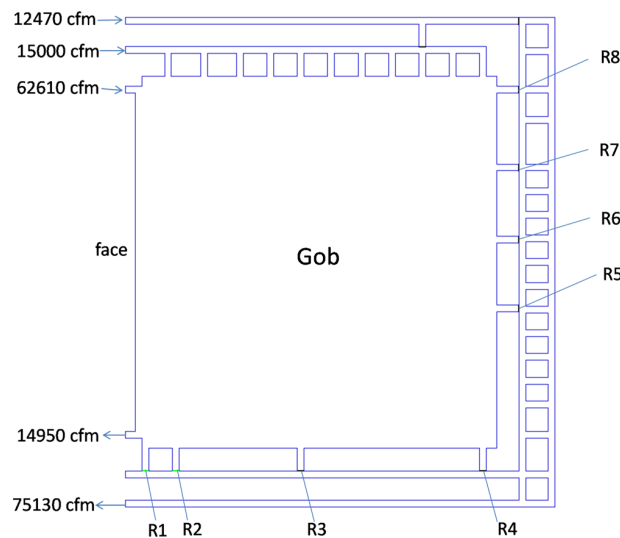
As the long-wall face progressed, a spontaneous heating occurred somewhere in the long-wall gob area, indicated by rising CO levels measured daily at the regulators. At that point, the ventilation scheme was changed over to a bleederless system in an attempt to control the heating event. Figure 2 shows the layout of the panel in the bleederless ventilation system configuration. Gob isolation seals were installed at crosscuts between the first and the second entries on the head-gate side. On the tailgate side, mainline seals were installed just in by the active long-wall face in the second entry to seal off the gob. The gob area is 1950 m (6500 ft) long, 375 m (1250 ft) wide and 10 m (33 ft) high. On the head-gate side, only the

first entry was considered and it was assumed to contain partially crushed coal pillars. On the tailgate side, the first and second entries were considered. The first entry was assumed to contain crushed coal pillars, whereas the second entry was assumed to be fully open.

Figure 2 Layout of long-wall panel with bleederless ventilation system (see online version for colours)
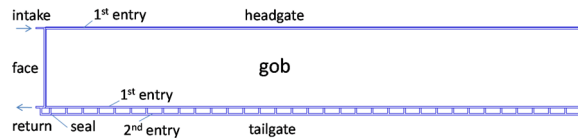
3 Modelling of spontaneous heating of coal

The chemical reaction between coal and oxygen at low temperatures is complex and still not completely understood. The following physical and chemical processes are believed to be involved: oxygen is transported to the surface of coal particles and into the coal pores. This results in a chemical interaction between coal and O_2 resulting in the release of heat and emission of gaseous products (Wang et al., 2003). The general chemical reaction between coal and O_2 can be expressed as

$$Coal + O_2 \rightarrow CO + CO_2 + H_2O + \text{other hydrocarbons} + \text{heat}.$$
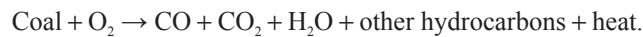
In this study, only CO and CO_2 are considered gaseous oxidation products and the chemical reaction between coal and oxygen is simplified as

$$Coal + O_2 \rightarrow aCO_2 + bCO + \text{heat}.$$

where a and b are the stoichiometric coefficient for CO_2 and CO, respectively. Based on laboratory-scale experiments conducted to determine the stoichiometric coefficients of the coal oxidation for coal from the mine in this study, the approximate values for 'a' and 'b' are 0.15 and 0.03, respectively. The rate of oxidation is dependent on temperature and oxygen concentration and is expressed in the form

$$\text{Rate} = A[O_2]^n \exp(-E/RT)$$

where the chemical reaction rate is defined as the rate of change in the concentrations of the reactants and products, A is the pre-exponential factor (K/s), E is the apparent activation energy (kJ/mol), R is the gas constant, n is the apparent order of reaction, T is the absolute temperature (°K) and $[O_2]$ is the oxygen concentration (kmol/m^3). The value of the apparent order of the reaction, n, in low-temperature oxidation studies of coal and other carbonaceous materials has been shown to vary from ~0.5 to 1.0 (Carras and Young, 1994) and is about 0.61 for US coals (Schmidt and Elder, 1940). The activation energy and pre-exponential factor for the coal were measured in laboratory-scale experiments as described elsewhere (Yuan and Smith, 2011). The activation energy, pre-exponential factor and other kinetic and physical properties for the coal are listed in Table 1. Coal oxidation is an exothermic reaction and the heat generated from the oxidation in the gob area is

dissipated by conduction and convection, whereas the oxygen and the oxidation products are transported by convection and diffusion.

Table 1 The physical and kinetic properties of the coal layer

Coal density	1300	kg/m^3
Coal specific heat	1003.2	J/kg-K
Coal conductivity	0.1998	W/m-K
Heat of reaction	300	kJ/mol-O$_2$
Activation energy	39.7	kJ/mol
Pre-exponential factor	5.9×10^4	K/s
Initial coal temperature	300 (27)	°K (°C)

To simulate the spontaneous heating of coal in long-wall gob area, the source of coal needs to be defined. The coal source can be coal left from the roof and from the mined coal seam or other overlying or underlying coal seams. An overlying rider coal seam may cave into the gob after the main coal seam is mined out while underlying rider coal seam may be exposed to the gob ventilation after floor heaves. Crushed coal pillars along the perimeter of the gob are also considered a coal source for spontaneous heating. The oxidation of coal can occur on any available coal surface including both external and internal pore surfaces. The available surface area for oxidation depends on the particle size distribution of the coal in the gob. It is difficult to define a coal particle size distribution in the coal layer in the gob area or crushed coal pillars because of the complexity of the gob. In these simulations, the available coal surface area is estimated by matching the predicted CO concentrations at three regulators with the measured CO data.

4   Numerical modelling

A commercially available CFD software program, FLUENT[1] from Ansys, Inc., was used in this study to simulate the gas flow and spontaneous heating in the long-wall gob area. The gas flow in the long-wall gob area was treated as laminar flow in a porous media using Darcy's law, whereas the gas flow in the ventilation airways was simulated as fully developed turbulent flow. The airflow rates for the bleeder ventilation system, shown in Figure 1, are used as boundary conditions for the simulations. For the bleederless ventilation system, mine ventilation data was also used as boundary conditions in the simulations. The pressure was –0.747 kPa (–3.0 inches water gauge) at the intake inlet, –0.872 kPa (–3.5 inches water gauge) at the return outlet. The intake airflow rate was 30 m^3/s (64,000 cfm). The long-wall face is assumed stationary during the simulations for both bleeder and bleederless ventilation systems.

The permeability and porosity distributions of the gob are also used as the boundary conditions for the simulations. For a fully compacted gob, the permeability and porosity distributions of the gob can be estimated based on geotechnical modelling of long-wall mining and the associated stress–strain changes using Fast Lagrangian Analysis of Continua (FLAC) code (Esterhuizen and Karacan, 2007). For a typical fully compacted long-wall panel, the permeability values in the gob area are estimated to vary from 3.0×10^4 to 8.5×10^5 MilliDarcies (MD), whereas the porosity value varies from 0.17 to 0.41 based on the modelling result from FLAC. Around the perimeter of the gob and immediately behind

the face shields, the permeability and porosity values are the largest, whereas near the centre of the gob, these values are the smallest due to compaction. The porosity profile in the gob is similar to the permeability profile. It is assumed that these permeability and porosity files do not change with the gob height.
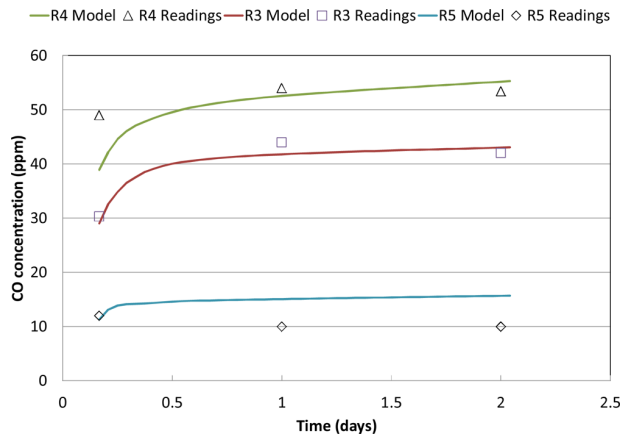
5   Simulation results and discussion
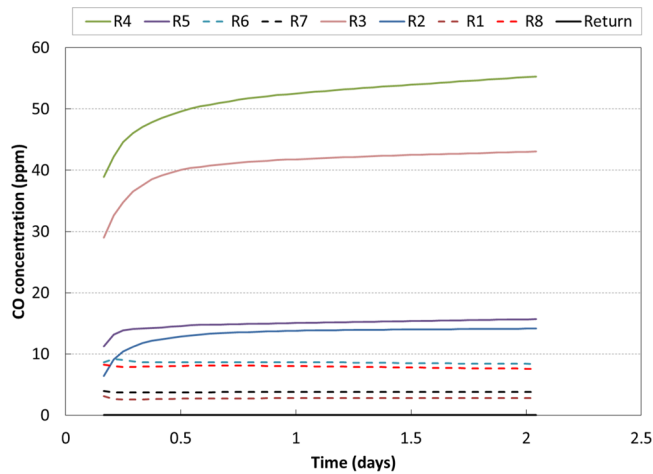
5.1   Bleeder ventilation system

Simulations were first conducted for the long-wall panel using the bleeder ventilation system as shown in Figure 1. Because of the short length of the panel, the gob would not be fully compacted. It can be seen from the ventilation data that 29.5 m^3/s (62,610 cfm) air entered the face entry, only 7 m^3/s (14,950 cfm) air exited the face into the return airway. Because there is no methane emission in this mine, methane dilution is not an issue. The remainder entered the gob and exited through the regulators. This indicates a higher gob permeability compared with fully compacted gob simulations. In the simulation, four measured intake airflow rates were used as the inlet boundary conditions. Different gob permeability values were simulated for the gob and the crushed coal pillars along the perimeter of the gob until the calculated outlet airflow rates converged to the measured values. After the two outlet airflow rates were matched with the measured values, simulation of coal oxidation was conducted. There is no overlying rider coal seam above this panel and the seam is mined floor to roof. The mine company reported that no coal was left on the roof and the floor. The only possible coal sources for spontaneous heating are crushed coal pillars at the back end and on the tailgate and head-gate sides of the panel. The broken coal from crushed pillars is normally in large size. However, for a reactive coal containing an easily fractured vertical cleat, which creates a multitude of airflow paths through it, it is likely for a potential self-heating to occur inside the large-size coal, as reported by Timko and Derick (1995). Normally, a thin layer (about 1 inch) can be left on the floor and likely stay in the gob. However, it is not likely for the coal to have a self-heating because the heat from the coal oxidation will be lost very quickly to the surroundings due to the small thickness of the coal layer, about 1 inch. The coal surface area available for coal oxidation in the crushed coal pillars is not known. In the next simulations, different coal surface area values were introduced to vary the degree of pillar crushing along the gob boundary until the calculated CO values converged to the measured values at regulators R3, R4 and R5. The CO concentrations at these three regulators were obtained daily and produced the largest measured CO concentrations. The solution indicated that the coal surface area on the head-gate side was about five times less than the surface area on the tailgate side and the back end, indicating a much smaller degree of coal pillar crushing on the head-gate side.

Figure 3 shows the comparison between the predicted CO values and measured CO values at those three regulators over a three-day period. At R3 and R4, the predicted CO values match very well with the measured values. At R5, the model shows slightly higher predicted CO values than the measured values. Overall, the model shows very good agreement with the measured values. Figure 4 shows the predicted CO values at all eight regulators and in the return. It is evident that for CO detection under these conditions, regulators 3 and 4 would give the earliest and the most reliable indication of a gob self-heating.

Figure 3 Comparison between calculated and measured CO values at three regulators (see online version for colours)

Figure 4 Calculated CO values for eight regulators and return (see online version for colours)


5.2 Bleederless ventilation system

Based on the validation of the CFD model and the calculation of the CO generation rates of the spontaneous heating process, simulations were then conducted for the long-wall panel using the bleederless ventilation system as shown in Figure 2 to determine optimum sampling locations for early detection of spontaneous combustion. The length of the panel is 1950 m (6500 ft); therefore, the gob would be considered fully compacted. The gob permeability and porosity distributions discussed in Section 3 are used in the simulations. Possible coal sources for oxidation in the gob are the crushed coal pillars at the back end of the panel and at the head-gate and tailgate sides. Also, in this simulation, a possible overlying rider coal seam caving into the gob is included in the model. The coal surface area determined in the simulation with the bleeder ventilation system was also used in these simulations. Based on the different coal sources, simulations were conducted for five coal source scenarios as shown in Table 2.

Table 2 Simulation coal source scenarios

Case	Coal source scenario
Case 1	crushed coal pillars on headgate, tailgate and backend
Case 2	crushed coal pillars on tailgate and backend
Case 3	caved rider coal seam, crushed coal pillars on headgate, tailgate and backend
Case 4	caved rider coal seam, crushed coal pillars on tailgate and backend
Case 5	caved rider coal seam

To evaluate the optimum location strategies for the early CO detection in the bleederless system, eight sampling points from a tube bundle system are considered in the simulations. Figure 5 shows the locations of these sampling points, designated as Line 1–8. The detailed positions of these points are given in Table 3. Lines 1, 3 and 4 are located in the second entry on the tailgate side. Lines 5 and 6 are behind the shields and lines 7 and 8 are located in the first entry on the head-gate side.

Figure 5 Locations of sampling points in bleederless ventilation system (see online version for colours)
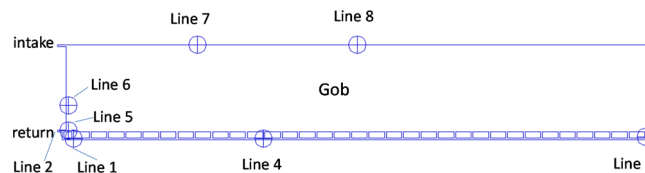
Table 3 Locations of sampling positions

Sampling position	Location
Line 1	immediately inby behind the mainline seal
Line 2	return
Line 3	original regulator 4 in bleeder system
Line 4	677 m from longwall face at tailgate side
Line 5	3 m from return corner and behind shields
Line 6	90 m from return corner and behind shields
Line 7	447 m from longwall face at headgate side
Line 8	1000 m from longwall face at headgate side

Figure 6 shows CO concentrations at the eight sampling locations for case 1, where the coal sources are crushed coal pillars along the head gate, tail gate and back end of the panel. The CO concentrations at lines 7 and 8, located along the head gate in the gob, continually increased and reached 1000 ppm in 5 days, whereas CO concentration increased to 180 ppm at line 4 and to 110 ppm at line 1 on the tailgate side. Figure 7 shows the CO concentration distribution in the gob area based on the model. Because the coal source was available only from the crushed pillars surrounding the gob and because of the lower permeability of the caved gob, the produced CO was found close to these pillars and was not transported deeper into the gob. The maximum predicted CO concentration in the gob was over 2000 ppm and occurred near the back end of the panel. However, these higher CO concentration values could not be detected at lines 3 and 4, probably because of weak gas flow in the gob.

The simulation results indicate that if the only coal source is the pillars surrounding the gob, the optimum sampling locations for the early detection are on the head-gate side.

Figure 6 CO concentrations at eight sampling positions for case 1 (see online version for colours)
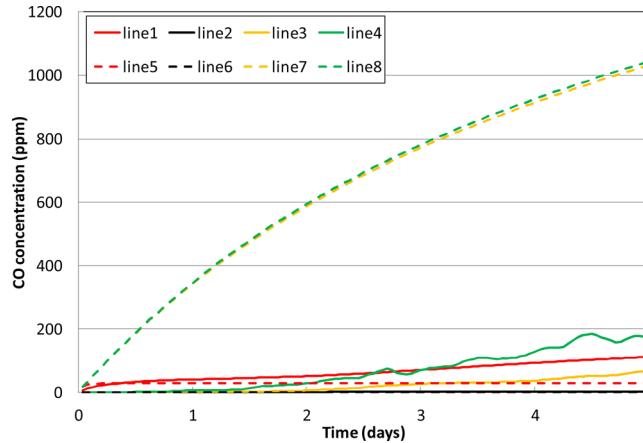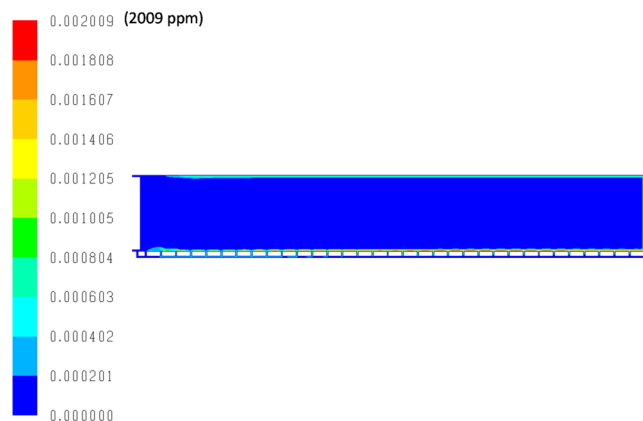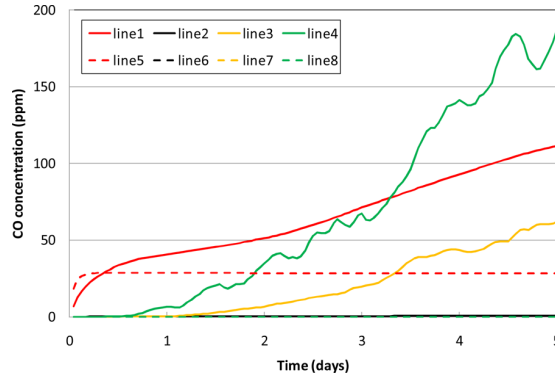

Figure 8 shows CO concentrations at eight sampling positions for case 2, where the coal sources are crushed coal pillars along the tail gate and back end of the panel. Because there are no crushed coal pillars on the head-gate side, no CO was found on the head-gate side. At the tailgate side, CO concentrations were much lower compared with the CO values at the head-gate side for case 1. The CO concentrations after 5 days at lines 4, 1 and 3, located in the tail gate, were 185, 110 and 60 ppm, respectively. The CO concentration distribution in the gob based on the model, shown in Figure 9, shows that the maximum CO concentration value in the gob was actually nearly the same as in Figure 7, near the pillars in the back end and back tailgate areas of the gob. However, lines 1 and 4 showed much lower CO values compared with the maximum value, 2010 ppm, probably because the sampling positions are in the second entry on the tailgate side, whereas the maximum values were in the caved first entry. The simulation results indicate that the optimum locations for early detection when a coal source is only available at the back and on the tailgate side are the sampling positions on the tailgate side, lines 4 and 1.

Figure 7 CO concentration distribution in the gob area for case 1 (see online version for colours)

Figure 8 CO concentrations at eight sampling positions for case 2 (see online version for colours)

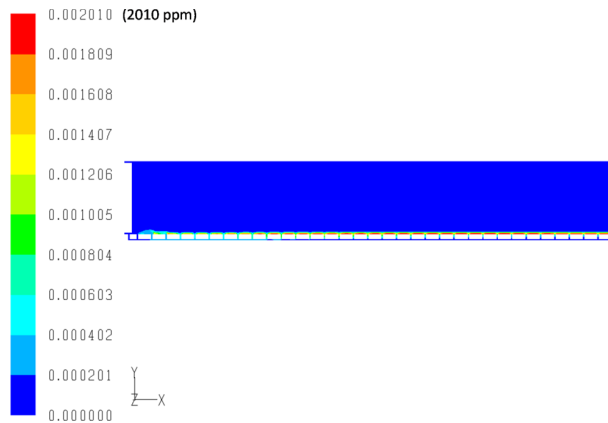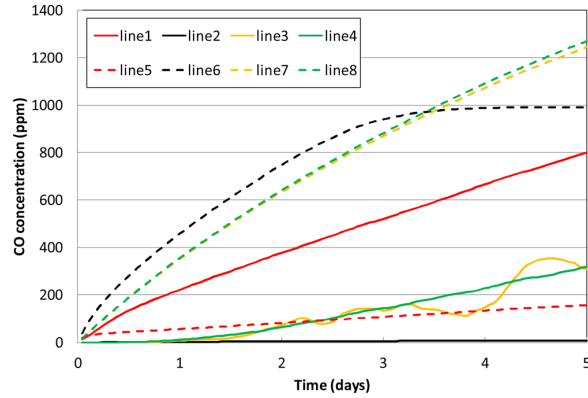**Figure 9** CO concentration distribution in the gob for case 2 (see online version for colours)


Figure 10 shows the CO concentrations at the eight sampling positions for case 3, where in addition to the pillars surrounding the gob, a caved rider seam also provides a coal source. The CO concentrations at lines 7 and 8 in the head gate continually increased to over 1200 ppm in 5 days, whereas the CO concentration increased to about 1000 ppm at line 6 just behind the shields and 800 ppm at line 1 just in by the face. Figure 11 shows the simulated CO concentration distribution in the gob area. The highest CO concentration, 2910 ppm, was at the centre of the gob because the CO generated from oxidation of rider seam coal was not transported easily out due to the lowest permeability there. The simulation results indicate that the optimum locations for early detection are the sampling positions on the head gate side and on the face when the coal source includes a caved rider and the crushed coal pillars along the perimeter of the gob.

Figure 12 shows CO concentrations at the eight sampling positions for case 4, where coal is present along the back and tail gate, as well as in a caved rider seam. The CO concentration at line 6 behind the shields increased to about 990 ppm in 5 days. The CO at the tailgate location increased to over 800 ppm at line 1, 312 ppm at line 4 and 245 ppm at line 3. On the head-gate side sampling locations at lines 7 and 8, the CO increased to 245 and 265 ppm, respectively. Figure 13 shows the simulated CO concentration distribution in the gob. Although the maximum CO concentration was nearly the same as in Figure 11, lines 7 and 8 showed much lower CO values because there was no coal available on the head-gate
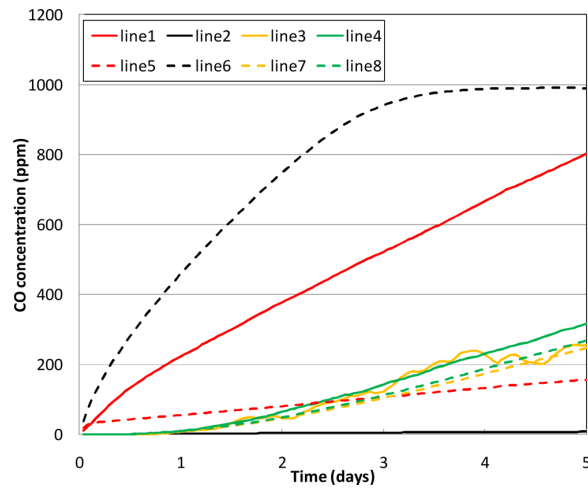
Figure 10 CO concentrations at eight sampling positions for case 3 (see online version for colours)

Figure 11 CO concentration distribution in the gob area for case 3 (see online version for colours)
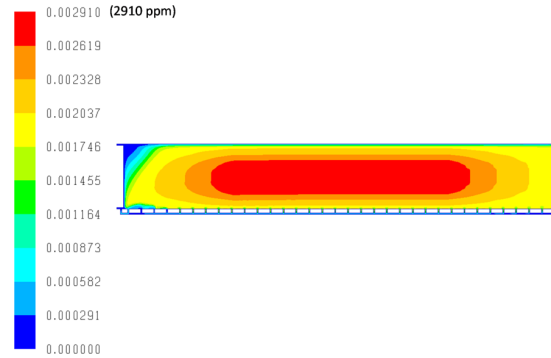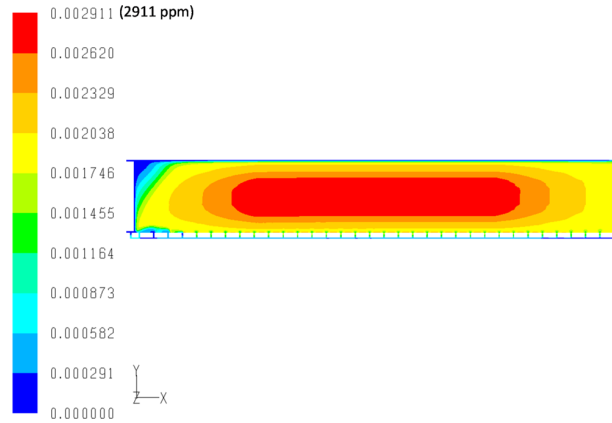

Figure 12 CO concentrations at eight sampling positions for case 4 (see online version for colours)


side. The simulation results indicate that the optimum locations for early detection in this scenario are the sampling positions on the face and on the tailgate side close to the face.

Figure 13 CO concentration distribution in the gob for case 4 (see online version for colours)

In the last simulation, the coal source was only a caved rider seam in the gob. Figure 14 shows CO concentrations at the eight sampling positions. The CO concentration at line 6, behind the shields, increased to about 990 ppm in 5 days. The CO at line 1 in the tail gate increased to 700 ppm, whereas lines 7 and 8 on the head-gate side increased to 240 and 260 ppm, respectively. It can be seen that CO concentration at line 6 is the same as for cases 3 to 5, indicating that it is from the oxidation of rider seam coal only. Results indicate that the optimum locations for early detection when only a rider seam is present are the sampling positions on the face and on the tailgate side close to the face.

Figure 14 CO concentrations at eight sampling positions for case 5 (see online version for colours)
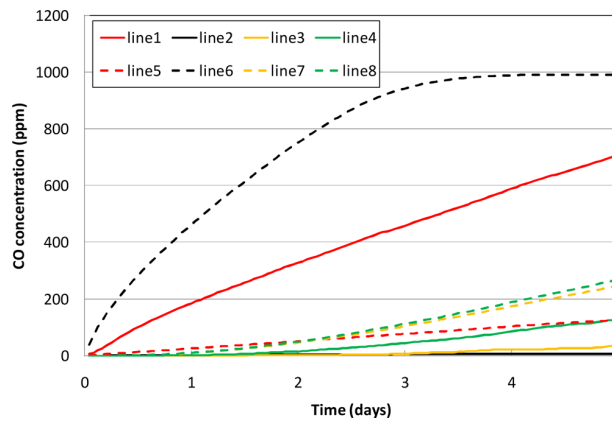
6 Conclusion

CFD simulations were conducted to investigate the optimum sampling locations when utilising a tube bundle system for early detection of spontaneous heating in a long-wall gob area. For the long-wall gob under bleeder ventilation conditions, simulation results demonstrate the optimum locations are the regulators on the tailgate side and close to the back end. The return is the least effective sampling location.

For the long-wall gob with a bleederless ventilation system, the optimum locations depend on the possible coal source location. When coal is available on the perimeter of the gob from the crushed coal pillars, sampling positions on the head-gate side are the optimum locations. If there is rider coal seam caving into the gob, sampling positions behind the shields are the optimum locations.

If crushed coal is available on the back end and tailgate perimeter of the gob but not on the head-gate side and there is no rider coal seam caving into the gob, the sampling positions on the tailgate side and close to the return are the optimum locations.

As with the bleeder ventilation system, the sampling location at the return is the least-effective sampling location for early detection of spontaneous heating under all coal source scenarios considered in the study.

Disclaimer: The findings and conclusions in this report are those of the authors and do not necessarily represent the views of the National Institute for Occupational Safety and Health.

References

Carras, J.N. and Young, B.C. (1994) 'Self-heating of coal and related materials: models, application and test methods', *Progress in Energy and Combustion Sciences*, Vol. 20, pp.1–15.

Chakravorty, R.N. and Woolf, R.L. (1979) 'Evaluation of systems for early detection of spontaneous combustion in coal mines', *Proceedings of the 2nd Mine Ventilation Congress*, Reno, Nevada, pp.1–5.

Chamberlain, E.A. and Hall, D.A. (1973) 'Practical early detection of spontaneous combustion', *Colliery Guardian*, Vol. 221, pp.190–194.

Cliff, D., Clarkson, F., Davis, R. and Bennett, T. (2000) 'The implications of large scale tests for the detection and monitoring of spontaneous combustion in underground coal', *2000 Queensland Mining Industry Health and Safety Conference*, Queensland, Australia, pp.27–30.

Esterhuizen, G.S. and Karacan, C.Ö. (2007) 'A methodology for determining gob permeability distributions and its application to reservoir modeling of coal mine longwalls', *SME 2007 Annual Meeting*, Denver, CO. Preprint 07-078.

Mitchell, D.W. (1996) *Mine Fires Prevention, Detection, Fighting*, Intertec Publishing, Chicago, IL.

Schmidt, L.D. and Elder, J.L. (1940) 'Atmospheric oxidation of coal at moderate temperatures', *Industrial and Engineering Chemistry*, Vol. 32, pp.249–256.

Smith, A.C. and Yuan, L. (2008) 'Simulation of spontaneous heating in longwall gob area with a bleederless ventilation system', *Mining Engineering*, Vol. 60, No. 8, pp.61–66.

Timko, R.J. and Derick, L.R. (1995) 'Predicting spontaneous heating in coal mine pillars', *Proceedings of the 7th US Mine Ventilation Symposium*. Lexington, Kentucky, pp.173-178.

Wang, H., Dlugogorski, B.Z. and Kennedy, E.M. (2003) 'Coal oxidation at low temperatures: oxygen consumption, oxidation products, reaction mechanism and kinetic modeling', *Progress in Energy and Combustion Science*, Vol. 29, pp.487–513.

Yuan, L. and Smith, A.C. (2007) 'Computational fluid dynamics modeling of spontaneous heating in longwall gob areas', *Transactions of Society for Mining, Metallurgy and Explorations*, Vol. 322, pp.37–44.

Yuan, L. and Smith, A.C. (2011) 'The effect of ventilation on spontaneous heating of coal', *Journal of Loss Prevention in Process Industries*, Vol. 25, pp.131–137.

Note

[1]Reference to a specific product is for informational purposes and does not imply endorsement by NIOSH.